Am J Physiol Regul Integr Comp Physiol 311: R1032–R1044, 2016.
First published September 14, 2016; doi:10.1152/ajpregu.00326.2016.

Early postnatal amylin treatment enhances hypothalamic leptin signaling and neural development in the selectively bred diet-induced obese rat

Miranda D. Johnson,[1] Sebastien G. Bouret,[2,3] Ambrose A. Dunn-Meynell,[4] Christina N. Boyle,[5] Thomas A. Lutz,[5] and Barry E. Levin[6]

[1]*Department of Psychiatry and Behavioral Sciences, Johns Hopkins University School of Medicine, Baltimore, Maryland;* [2]*The Saban Research Institute, Developmental Neuroscience Program, Children's Hospital Los Angeles, University of Southern California, Los Angeles, California;* [3]*INSERM, Jean-Pierre Aubert Research Center, Lille, France;* [4]*Neurology Service, Veterans Administration Medical Center, East Orange, New Jersey;* [5]*Institute of Veterinary Physiology, University of Zurich, Zurich, Switzerland; and* [6]*Department of Neurology, Rutgers New Jersey Medical School, Newark, New Jersey*

Submitted 22 July 2016; accepted in final form 2 September 2016

Johnson MD, Bouret SG, Dunn-Meynell AA, Boyle CN, Lutz TA, Levin BE. Early postnatal amylin treatment enhances hypothalamic leptin signaling and neural development in the selectively bred diet-induced obese rat. *Am J Physiol Regul Integr Comp Physiol* 311: R1032–R1044, 2016. First published September 14, 2016; doi: 10.1152/ajpregu.00326.2016.—Selectively bred diet-induced obese (DIO) rats become obese on a high-fat diet and are leptin resistant before becoming obese. Compared with diet-resistant (DR) neonates, DIO neonates have impaired leptin-dependent arcuate (ARC) neuropeptide Y/agouti-related peptide (NPY/AgRP) and α-melanocyte-stimulating hormone (α-MSH; from proopiomelanocortin (POMC) neurons) axon outgrowth to the paraventricular nucleus (PVN). Using phosphorylation of STAT3 (pSTAT3) as a surrogate, we show that reduced DIO ARC leptin signaling develops by postnatal day 7 (P7) and is reduced within POMC but not NPY/AgRP neurons. Since amylin increases leptin signaling in adult rats, we treated DIO neonates with amylin during postnatal hypothalamic development and assessed leptin signaling, leptin-dependent ARC-PVN pathway development, and metabolic changes. DIO neonates treated with amylin from P0–6 and from P0–16 increased ARC leptin signaling and both AgRP and α-MSH ARC-PVN pathway development, but increased only POMC neuron number. Despite ARC-PVN pathway correction, P0–16 amylin-induced reductions in body weight did not persist beyond treatment cessation. Since amylin enhances adult DIO ARC signaling via an IL-6-dependent mechanism, we assessed ARC-PVN pathway competency in IL-6 knockout mice and found that the AgRP, but not the α-MSH, ARC-PVN pathway was reduced. These results suggest that both leptin and amylin are important neurotrophic factors for the postnatal development of the ARC-PVN pathway. Amylin might act as a direct neurotrophic factor in DIO rats to enhance both the number of POMC neurons and their α-MSH ARC-PVN pathway development. This suggests important and selective roles for amylin during ARC hypothalamic development.

leptin; amylin; NPY; AgRP; POMC; hypothalamus

DURING HYPOTHALAMIC DEVELOPMENT in the rodent, leptin serves as a crucial neurotrophic factor important for the establishment of neuronal pathway projections from the arcuate nucleus (ARC) to the paraventricular nucleus of the hypothalamus (PVN) (6). Leptin exerts opposing effects on ARC neuropeptide Y/agouti-related peptide (NPY/AgRP) and proopiomelanocortin (POMC) neurons post-weaning, hyperpolarizing the former while depolarizing the latter to release α-melanocyte stimulating hormone (α-MSH). However, before the maturation of ATP-sensitive K^+ channels on NPY/AgRP neurons (3), leptin promotes axonal outgrowth from both neuronal populations to the PVN and other target areas. In addition, as occurs in the *ob/ob* mouse, the absence of leptin during the first 2 wk of life results in diminished neuronal pathway development that can only be rescued if leptin is given exogenously during this critical period (6). When placed on a 32% fat high-energy (HE) diet, the selectively bred diet-induced obese (DIO) rat rapidly becomes hyperphagic and obese. Prior to becoming obese, the DIO rat has early deficits in leptin receptor (Lepr-b) signaling, which include reduced Lepr-b mRNA expression (22), leptin binding to its receptor (16), and impaired leptin-induced expression of phospho-STAT3 (pSTAT3) in the ARC at postnatal day 10 (P10) (8). In keeping with their early-onset deficits in leptin signaling, DIO neonates also have defective ARC-to-PVN pathway development (8), which normally is fully developed in rodents by P14 (6).

Amylin is co-released with insulin from pancreatic β-cells in response to a meal and rising blood glucose levels (17, 26). Amylin acts on its receptor, which is a heterodimeric receptor complex composed of a calcitonin receptor (CTR) core (CTR1a or -b) combined with one of three receptor activity-modifying proteins (RAMP1–3) (14). Components of the amylin receptor are widely expressed throughout the brain (5, 18, 38, 47). Amylin produces satiation by acting directly on its receptor in the area postrema (AP), a circumventricular organ, which has no blood-brain barrier and where all amylin receptor components are expressed in single cells (4, 25, 28). However, amylin also crosses the blood-brain barrier (1, 2) which presumably underlies the ability of exogenously administered amylin to increase leptin signaling in the ventromedial nucleus of the hypothalamus (VMN) of adult rats (43, 45). Furthermore, in adult DIO rats, pretreatment with amylin for 7 days restored their impaired leptin signaling in the VMN (35). Recently, we demonstrated that amylin enhances leptin signaling in the ventromedial hypothalamus (VMH: ARC + VMN) by stimulating microglia to produce interleukin-6 (IL-6) (18). This amylin-induced microglial release of IL-6 acts on its IL-6/gp130 receptor complex on VMH neurons to enhance leptin-induced phosphorylation of STAT3 downstream of both the IL-6 receptor complex and Lepr-b (18). Given the defective development of both AgRP and α-MSH ARC-PVN pathways associated with impaired leptin signaling in DIO neonates (8) and the fact that amylin enhances leptin signaling in adult DIO rats (35), we hypothesized that DIO rats might have an inborn deficit in the postnatal development of leptin-dependent ARC

Address for reprint requests and other correspondence: B. E. Levin, 39 Donna Dr., Bloomfield, NJ 07003 (e-mail: levin@njms.rutgers.edu).

NPY/AgRP and POMC neuronal migration (8) compared with DR rats, and that administration of exogenous amylin to DIO neonates during the first 2 wk of critical hypothalamic development would correct these deficits, as well as rescue their defective ARC-PVN pathway outgrowth of AgRP and α-MSH neurons.

MATERIALS AND METHODS

Animal Husbandry and Diet

Selectively bred DIO and DR dams (20) were raised in our vivarium and fed ad libitum on chow diet (#5001; Purina, St. Louis, MO) containing 3.35 kcal/g with 29.8% protein, 13.5% fat, and 56.7% carbohydrate as a percentage of total energy content throughout gestation and lactation. For all studies, litters were normalized to 10 pups/litter (6 males: 4 females) on P0 (defined as the first 24 h of birth). Only male DIO and DR rats were used for all experiments. Experimental groups contained 7–8 pups, a number based on our own previously published developmental experiments (8, 11, 12). For the neonatal IL-6 knockout (KO) study, 8-wk-old male and female IL-6 KO (B6;129S6-Il6tm1Kopf/J) and wild-type (wt) (C57BL/6J) mice were purchased from The Jackson Laboratory (Bar Harbor, ME) and fed mouse chow (Purina #5015; 3.81 kcal/g, 25% fat, St. Louis, MO). After a 1 wk acclimation period, mice were bred and litters were then culled to 6–7 pups/litter. Only male IL-6 KO and wt neonates were used and experimental groups contained 6–7 pups. All animals were maintained on a reversed 12:12-h light-dark schedule with lights off at 0800 (8:00 AM) with food and water provided ad libitum. All work was approved by the Institutional Animal Care and Use Committee of the East Orange Veterans Affairs Medical Center (East Orange, NJ).

Experiment 1: Leptin Signaling in the ARC of DIO and DR Neonates

Assessment of the number of ARC NPY and POMC neurons during the first week of the postnatal hypothalamic developmental period was performed at P0, 4, and 7 in male DIO and DR neonates, which were euthanized by perfusion (n = 7–8/group/age). Neonates were injected with leptin for the assessment of leptin-induced pSTAT3 expression as a surrogate for leptin signaling by double-label immunohistochemistry (IHC) with POMC or with NPY in situ hybridization (ISH).

Experiment 2: Effects of Postnatal Amylin Treatment in DIO Neonates

Male DIO neonates were weighed and injected (ip) three times daily, (during the dark cycle in 4-h increments) from either P0–6 or P0–16 (where indicated) with amylin (100 μg/kg 3× a day; Bachem, Torrance, CA, dissolved in 0.9% saline) or 0.9% saline alone (n = 8/treatment with 1 saline- and 1 amylin-treated/litter, i.e., 1 treatment/litter) for a total volume injection of 0.1 ml (P0–6) or 0.2 ml (P7–P16).

Experiment 2.1. DIO neonates were treated daily with saline or amylin from P0–6 (n = 8/treatment, 1 treatment/litter). On P7, saline- and amylin-injected DIO neonates were killed for leptin-induced pSTAT3 with double-labeling for POMC or NPY.

Experiment 2.2. DIO neonates were given amylin or saline from (P0–16) and then divided into two groups on P17 (n = 16/treatment, 2/treatment/litter). *Group 1* (n = 8/treatment) neonates were euthanized for leptin-induced pSTAT3 IHC, and *group 2* (n = 6/treatment) neonates were assessed for ARC-PVN neuronal pathway development by AgRP/α-MSH IHC.

Experiment 2.3. DIO neonates were injected with amylin or saline from P0 to P16 (n = 8/treatment, 1 treatment/litter). On P21, neonates were weaned and placed on chow. Cumulative body weight and food intake measurements were collected weekly during the experiment. During the 4th postweaning week on chow, food was removed 2 h before lights out (0600). At lights out (0800), rats were randomized and given an injection of leptin (5 mg/kg ip; National Hormone and Peptide Program, Torrance, CA) in 0.4 ml of phosphate-buffered saline (PBS) or PBS alone, and food was returned. Food intake was monitored 4 and 24 h later to determine leptin-induced anorexia. Three days later, the treatments were reversed, and food intake was again monitored. After 5 wk on chow diet, rats were assessed for leptin signaling in the ARC and VMN by leptin-induced pSTAT3 IHC.

Experiment 2.4. DIO neonates were injected with amylin or saline from P0–16 and weaned onto chow at P21 (n = 13/treatment, 2 treatment/litter). Cumulative body weight and food intake measurements were collected weekly during the experiment. After 4 wk on chow, rats underwent an oral glucose tolerance test (OGTT). During *week 5* on chow, rats were divided into two groups. *Group 1* rats (n = 8/treatment) were euthanized by rapid decapitation at lights out (0800) in a nonfasted state, and brains were assessed for ^{125}I-labeled leptin receptor binding autoradiography in the ARC and VMN. Adiposity was assessed by weighing five representative fat pads (retroperitoneal, inguinal, epididymal, mesenteric, and perirenal) and expressing these weights as percent total body weight. *Group 2* rats (n = 5/treatment) were fed chow for 5 wk after weaning and then placed on HE diet for an additional 8 wk. The HE diet contains 4.47 kcal/g with 21% protein, 32% fat, and 48% carbohydrate, 50% of which is sucrose (Research Diets no. C11024F, New Brunswick, NJ). During *week 7* on HE diet, rats underwent an OGTT. At the end of *week 8* on HE diet, rats were euthanized, and adiposity was assessed as above.

Experiment 3: Hypothalamic ARC-PVN Pathway Development in IL-6 KO Mice

We previously demonstrated that exogenous amylin administration stimulates VMH microglia to produce IL-6, which then acts to enhance leptin signaling in the ARC and VMN (18). In *experiment 2* above, we demonstrated that neonatal amylin treatment improved the defective leptin-dependent ARC-PVN AgRP and α-MSH pathway development of DIO rats (8). To assess the degree to which this amylin action might be dependent on activation of IL-6, P17 male IL-6 KO and WT mice were assessed for ARC-PVN neuronal pathway development by AgRP/α-MSH IHC (n = 6–7/genotype).

Leptin-Induced pSTAT3 Single- and Double-Label Immunohistochemistry

Food was removed 2 h before lights out (0600) in adult but not neonatal rats. At lights out (0800), rats were injected with leptin (5 mg/kg ip; National Hormone and Peptide Program, Torrance, CA) in 0.4 (adult) or 0.2 ml (neonate) of PBS. After 45 min, they were anesthetized with ketamine-xylazine and rapidly perfused with 0.9% saline followed by 2% paraformaldehyde (PFA). Brains were removed, postfixed for 1 h in 2% PFA, submerged overnight at 4°C in 20% sucrose, and sectioned at either 20 μm (neonates) or 25 μm (adults) serially through the ARC and VMN. Single-label pSTAT3 IHC was carried out as previously described, using rabbit anti-pSTAT3 antibody (1:1,000; Cell Signaling Technologies) (8, 9). Double-label pSTAT3-POMC IHC in neonatal tissue sections was carried out after incubation with rabbit anti-pSTAT3. Following incubation in CY3 donkey anti-rabbit for 2 h (1:250; Jackson ImmunoResearch) sections were incubated for 72 h in blocking solution containing rabbit anti-POMC antibody (1:1,000; Phoenix Pharmaceuticals). Following rinses, sections were placed in Alexa fluor 488 goat anti-rabbit for 2 h (1:250; Invitrogen) and coverslipped using Vectashield Hardset mounting medium.

NPY ISH and pSTAT3 IHC

Separate slide sets were used to perform combined NPY ISH and pSTAT3 IHC using modifications to Baquero et al. (3). NPY sense and antisense digoxigenin-labeled riboprobes were generated from plasmids containing inserts for mRNA of rat NPY (42) [GenBank no. M20373.1 bases 1–511, derived from original probe of Higuchi et al.

(15)]. After hybridization, slides were incubated with anti-digoxigenin-horseradish peroxidase (anti-DIG-POD,1:500; Roche) overnight at 4°C and then processed using TSA Plus CY3 Tyramide (NEL753001KT; PerkinElmer). The horseradish peroxidase signal was quenched using 1% H_2O_2 in PBS for 10 min. Sections were incubated overnight in block solution containing rabbit anti-pSTAT3 (1:500; Cell Signaling), incubated with biotinylated goat anti-rabbit (1:500, Vector Laboratories) and processed using TSA Biotin Tyramide (NEL700A001KT; PerkinElmer). Sections were then placed in streptavidin-Alexa fluor 488 conjugate (1:250; Invitrogen). Coverslips were applied with Vectashield Hardset mounting medium.

α-MSH and AgRP IHC

α-MSH and AgRP IHC was performed using previously described methods (8, 31). At lights out (0800), neonates were injected with ketamine-xylazine and perfused with 0.9% saline followed by 4% PFA in borate buffer. Brains were then postfixed in 4% PFA borate buffer containing 20% sucrose, submerged overnight at 4°C in 20% sucrose in 0.02 M KPBS, and frozen with 2-methylbutane. Brains were sectioned at 30 μm serially through the PVN. For α-MSH, sections were incubated overnight in LKPBS (0.3% Triton X-100 and 2% normal donkey serum in KPBS) containing sheep anti-α-MSH (1:40,000; Chemicon) for 72 h and visualized with Alexa fluor 568 donkey anti-sheep secondary antibody (1:200; Invitrogen). For AgRP, sections were incubated overnight in LKPBS (0.3% Triton X-100 and 2% normal goat serum in KPBS) containing rabbit anti-AgRP (1:4,000; Phoenix Pharmaceuticals) for 72 h. The signal was amplified using a TSA Biotin Tyramide kit (NEL700A001KT, PerkinElmer) and visualized with streptavidin-Alexa fluor 568 conjugate (1:1,000; Invitrogen). For both assays, sections were counterstained with bisbenzamide, and coverslips were placed using Vectashield mounting medium. Brains were analyzed for ARC-PVN fiber density as previously described (8, 31).

Quantitative Analysis of Immunolabeled Cells

Cells expressing pSTAT3, POMC, and NPY in the ARC (P0–17) and VMN (P17 neonates and adults) were imaged using an Optronics MagnaFire camera (Optotronics) attached to an Olympus BX60 microscope (Olympus). Images of single-labeled neurons and merged images of co-labeled neurons were counted by an experimentally naïve observer using Adobe Photoshop software to allow for quantification. For quantification of the ARC (P0–7), it was divided into the four divisions described by Palkovits (30) as determined by cresyl violet-stained sections at each postnatal age (Fig. 1). The numbers of cells counted within each division, as well as the combined total of all four divisions, were averaged and used for statistical comparisons. For each age quantified per IHC/ISH assay, a set number of sections was assigned to each division and matched between animals. For *divisions 1* (DIV1) and DIV2, two sections per division were counted. For DIV3, six were counted. Finally, for DIV4, two sections were counted. At P17, only three sections encompassing the midpoint of the ARC, VMN, and DMN, pars compacta as verified (Paxinos et al., 1986) were used for quantification.

For the quantitative analysis of α-MSH and AgRP fiber density, two sections through the PVH from animals of each experimental group were acquired using a Zeiss LSM 710 confocal system equipped with a ×20 objective. Slides were numerically coded to obscure the treatment group. Image analysis was performed using ImageJ analysis software (National Institutes of Health) as previously described (41). Briefly, each image plane was binarized to isolate labeled fibers from the background and to compensate for differences in fluorescence intensity. The integrated intensity, which reflects the total number of pixels in the binarized image, was then calculated for each image. This procedure was conducted for each image plane in the stack, and the values for all of the image planes in a stack were summed. The resulting value is an accurate index of the density of the processes in the volume sampled.

OGTT and Blood Analysis

For OGTT, food was removed 2 h before lights out (0600) and baseline samples from tail nick were collected at lights out (0800) into EDTA-coated tubes for glucose and insulin assays. Rats were then gavaged with 2 g/kg glucose and blood was collected at 15, 30, 60, 90, and 120 min via tail nick for insulin and glucose. Terminal blood samples for several studies were collected from trunk blood (food removed 2 h before lights out). For all samples, plasma was analyzed by radioimmunoassay using antibodies specific to rat insulin and leptin (Linco, Carlsbad, CA). Plasma glucose was measured using an Analox glucometer (San Diego, CA).

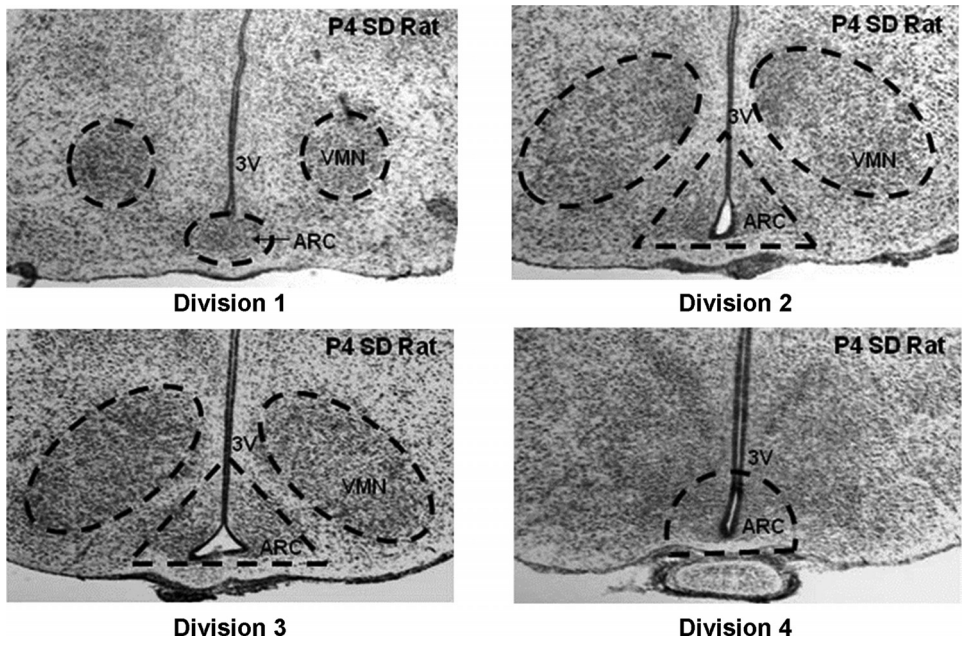

Fig. 1. Cresyl violet-stained sections through the rostral-caudal extent of the ARC in P4 outbred Sprague-Dawley rats. Divisions established by Palkovits (31). Abbreviations in figures: DIO, diet-induced obese; DR, diet resistant; HE, high energy; IHC, immunohistochemistry; ISH, in situ hybridization; α-MSH, α-melanocyte-stimulating hormone; POMC, proopiomelanocortin; NPY/AgRP, neuropeptide Y/agouti-related protein; IL-6, interleukin-6; IL-6R, IL-6 receptor; GP130, glycoprotein 130; Lepr-b, leptin receptor-b; CTR, calcitonin receptor core; RAMP, receptor activity-modifying protein; JAK/STAT3, Janus-activated kinase/signal transducer and activator of transcription 3; pSTAT3, phosphorylated STAT3; pERK, phosphorylated extracellular factor-regulated kinase; ME, median eminence; 3V, (3rd ventricle; ARC, arcuate nucleus of the hypothalamus; PVN, paraventricular nucleus of the hypothalamus.

Quantitative Leptin Receptor Binding Autoradiography

Binding of ^{125}I-labeled leptin to its cell surface receptors on ARC and VMN neurons was carried out as previously described (16). Both neonate and adult rats were euthanized by rapid decapitation at the onset of lights out (0800) in a nonfasted state. Brains were removed, snap-frozen on dry ice, cut in 16-μm serial sections, freeze-thawed onto gel-coated slides, desiccated overnight, and stored at −80°C. Slides were then thawed at room temperature, dipped in ice-cold 0.5% PFA, and dipped several times in ice-cold Tris·HCl (pH 7.2). Slides were then incubated with 0.25 nM murine ^{125}I-labeled leptin (PerkinElmer Life Sciences, Boston, MA) in Tris·HCl containing 1% BSA, 0.05% leupeptin, and 0.001% pepstatin for 1 h at room temperature. A 10-fold excess of unlabeled leptin (National Hormone and Peptide Program, Torrance, CA) in the presence of ^{125}I-labeled leptin was used to assess nonspecific "binding." Slides were then dipped in ice-cold Tris·HCl and incubated in 4% PFA, followed by a dip in ice-cold Tris·HCl. Slides were then dipped in ice-cold dH_2O, dried under forced cold air, and apposed to BioMax MR film (Kodak-Carestream, Rochester, NY) for 10 days. After developing, the autoradiograms were assessed by a computer-assisted densitometry system (Drexel) by a researcher naïve to the experimental groups using the cresyl violet-stained sections from which the autoradiograms were derived to define anatomic areas.

Statistical Analysis

Statistical comparisons among variables were made by two-sample *t*-test and 1- or 2-way ANOVA with Bonferroni post hoc correction for multiple comparisons, where appropriate. Body weight gain and food intake were analyzed by 1-way ANOVA with repeated measures. Calculations for area under the curve (AUC) were performed using the trapezoidal method with GraphPad Prism software. The insulin sensitivity index (29) was used to determine whole body insulin sensitivity after OGTT and is as follows: insulin sensitivity index (ISI) = 10,000/square root [(fasting glucose × fasting insulin) × (mean glucose × mean insulin)]. All data are expressed as means ± SE. Statistical analysis was performed by using SYSTAT software (SYSTAT, Chicago, IL) and graphs made using appropriate software (GraphPad Prism, La Jolla, CA).

RESULTS

Experiment 1: Ontology of DIO and DR Postnatal POMC and NPY Neuronal Leptin Signaling

At P0 and P4, DIO and DR neonates had the same number of leptin-induced pSTAT3-positive ("leptin-sensitive") neurons across the entire ARC extent (Fig. 2*A*), which was consistent across each individual division of the ARC (Fig. 3, *A–H*).

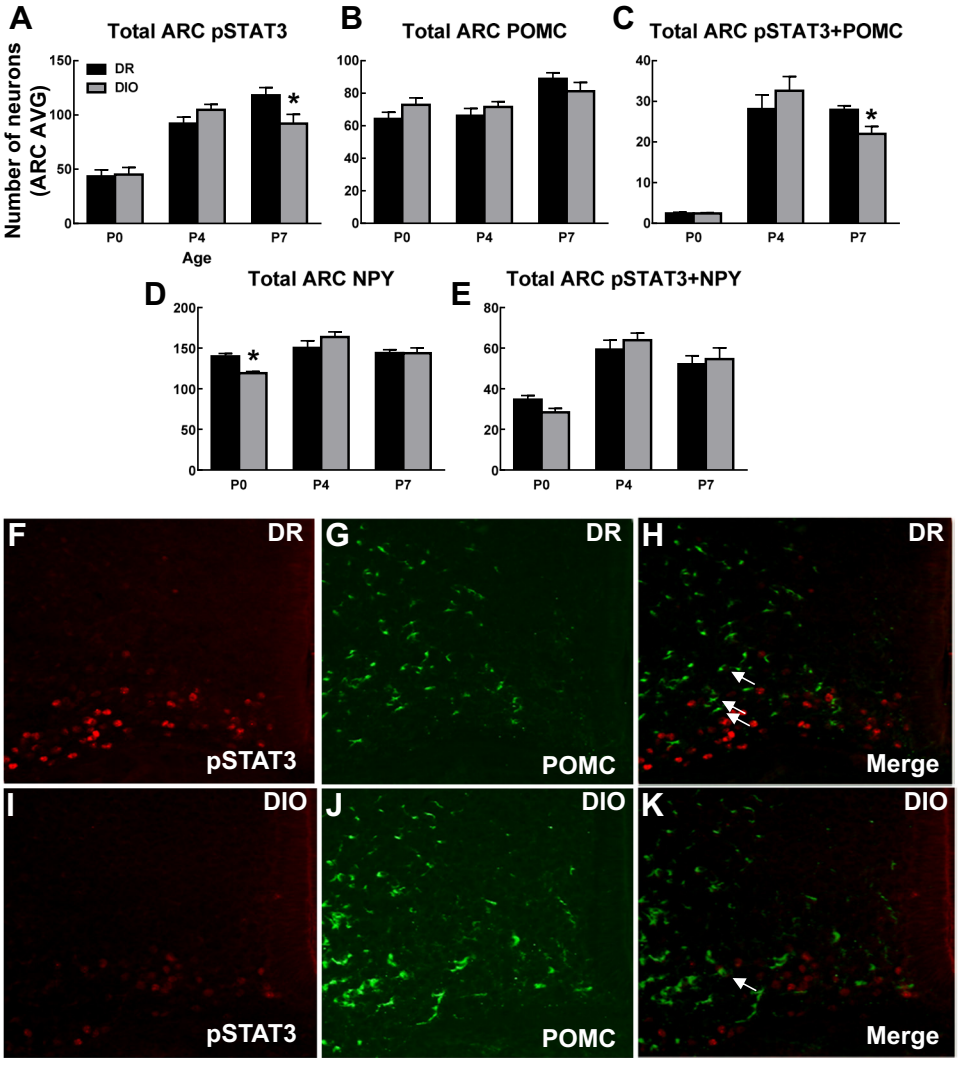

Fig. 2. Leptin-induced pSTAT3, POMC, NPY, and double-label IHC in the ARC of DIO and DR neonates at P0, P4, and P7. (*A*) leptin-induced pSTAT3 IHC, (*B*) POMC IHC, (*C*) leptin-induced pSTAT3+POMC IHC, (*D*) NPY ISH, and (*E*) leptin-induced pSTAT3+NPY IHC/ISH. Images (×20) of ARC *division 4* (DIV4) leptin-induced pSTAT3 (*F*, DR; *I*, DIO), POMC (*G*, DR; *J*, DIO) and leptin-induced pSTAT3+POMC (*H*, DR; *K*, DIO). White arrows denote leptin-induced pSTAT3+POMC-positive neurons. Data are expressed as means ± SE with average neuronal counts per section. *$P <$ 0.05 or less, two-sample *t*-test.

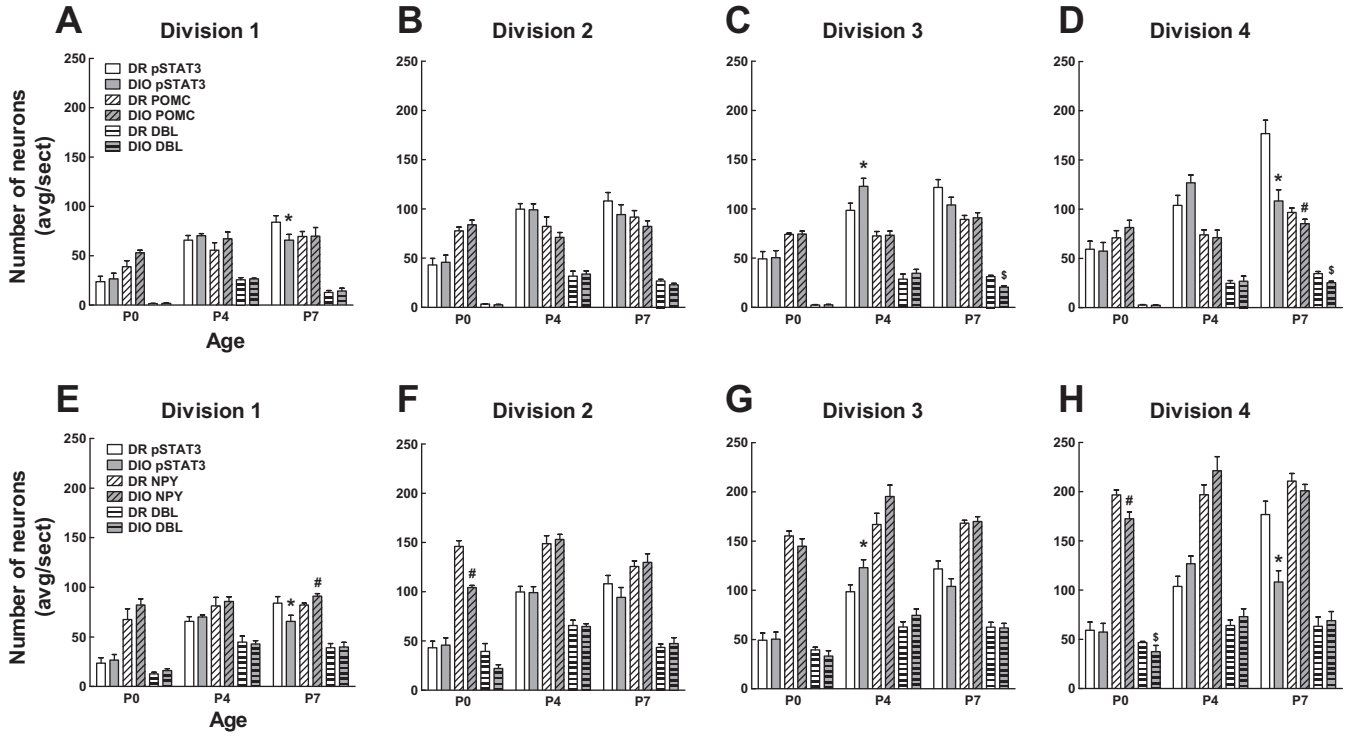

Fig. 3. Leptin-induced pSTAT3, POMC, NPY, and double-label IHC through the rostral-caudal extent of the ARC in DIO and DR neonates at P0, P4, and P7. *A–D*: leptin-induced pSTAT3 IHC, POMC IHC, and leptin-induced pSTAT3+POMC IHC in DIV1-rostral ARC (*A*), 2-rostral/mid ARC (*B*), 3-mid ARC (*C*), and 4-caudal ARC (*D*). *E–F*: leptin-induced pSTAT3 IHC, NPY ISH, and leptin-induced pSTAT3+NPY IHC/ISH in DIV1-rostral ARC (*E*), 2-rostral/mid ARC (*F*), 3-mid ARC (*G*), and 4-caudal ARC (*H*). Data are expressed as means ± SE with average neuronal counts per section. $^{*\#\$}P < 0.05$ or less, two-sample *t*-test. *DR vs. DIO leptin-induced pSTAT3; #DR vs. DIO POMC or NPY; $DR vs. DIO pSTAT3 POMC or NPY double-label neurons.

However, at P4, while DIO and DR neonates had the same number of leptin-sensitive neurons in the entire ARC (Fig. 2A), DIO rats had 25% more leptin-sensitive neurons selectively in the mid-ARC [*division 3* (DIV3), Fig. 3, *C* and *G*] than did DR neonates. By P7, DIO neonates had 22% fewer leptin-sensitive neurons in the entire ARC (Fig. 2*A*), with 22 and 39% fewer leptin-sensitive neurons in the rostral (DIV1, Fig. 3, *A* and *E*) and caudal ARC (DIV4, Fig. 3, *D* and *H*) than did DR neonates, respectively.

Although DIO and DR neonates had the same total number of ARC POMC neurons at all ages (Fig. 2*B*), DIO neonates had 22% fewer leptin-sensitive POMC neurons across the entire ARC expanse at P7 (Fig. 2*C*). Also, only at P7, DIO neonates had 12% fewer POMC neurons in the caudal ARC (DIV4, Fig. 3*D*). Of these POMC neurons at P7, 34 and 27% fewer were leptin sensitive in the mid- and caudal ARC, (DIV3 and 4, Fig. 3, *C* and *D*), respectively, than were those in DR neonates. As opposed to POMC neurons, DIO neonates had 15% fewer NPY neurons across the entire ARC at P0 (Fig. 2*D*). This was due primarily to a 29% reduction in DIV2 (Fig. 2*E*) and 12% reduction in DIV4 (Fig. 3*H*) at P0. However, this difference in total number of ARC NPY neurons did not persist at older ages, and DIO neonates actually had 11% more NPY neurons in DIV1 at P7 than did DR neonates (Fig. 3*E*). DIO and DR neonates had the same total number of ARC leptin-sensitive NPY neurons across all ages examined (Fig. 2*E*), although DIO neonates did have 19% fewer leptin-sensitive NPY neurons in the caudal ARC (DIV4, Fig. 3*H*) at P0. In agreement with previous findings (33), DIO and DR neonates did not differ in body weight or adiposity at these early ages (data not shown).

Experiment 2

Effects of P0–6 amylin treatment on DIO ARC leptin signaling. Because amylin increases VMH leptin signaling in adult DIO rats (18), we assessed whether amylin administration from P0–6 would similarly increase leptin signaling and ameliorate the abnormal ARC-PVN development of leptin resistant DIO rats (8, 21). Compared with controls at P7, amylin-injected rats had 8% more leptin-induced pSTAT3-positive neurons across the entire rostral-caudal extent of the ARC due to a 12 and 9% increase in *divisions 2* and *3*, respectively (Fig. 4*A*). Although amylin treatment increased the number of POMC neurons by 37% and 34% in *divisions 1* and *2* (Fig. 4*B*; DIV1 and -2), it had no effect on the number of leptin-sensitive POMC neurons compared with controls (Fig. 4*C*). As opposed to POMC neurons, which were increased by amylin treatment, this treatment had no effect on the number of NPY neurons (Fig. 4*D*); nor did it affect the number of leptin-sensitive NPY neurons compared with controls (Fig. 4*E*). These results suggest that, whereas early neonatal amylin treatment had a selective effect on increasing the number of leptin-sensitive ARC neurons, this amylin effect involved neither POMC nor NPY neurons.

Effects of P0–16 amylin treatment on DIO ARC leptin signaling, ARC-PVN pathway development, and body weight gain. When amylin treatment was extended from P0 to P16 in DIO neonates, they had 22 and 9% more leptin-induced pSTAT3-positive neurons at P17 in the ARC and VMN than controls, respectively (Fig. 5, *B–F*). These data confirm the fact that neonatal amylin treatment increases the number of leptin-

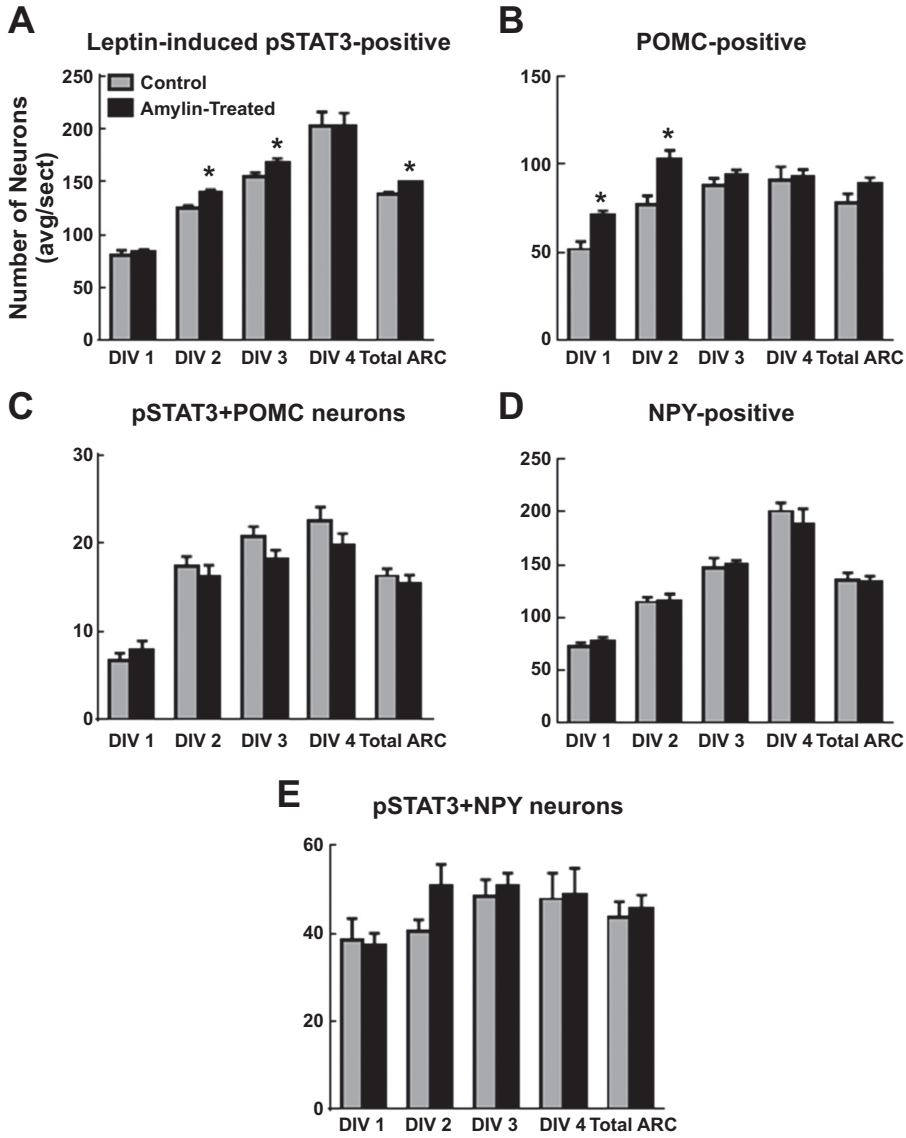

Fig. 4. ARC leptin receptor signaling in P7 DIO rats treated with amylin (300 μg ·kg^{-1} ·day^{-1}) vs. vehicle (0.9% saline) from P0 to P6. *A*: leptin-induced pSTAT3-positive, *B*: POMC-positive, *C*: leptin-induced pSTAT3+POMC double-label, *D*: NPY-positive, and *E*: leptin-induced pSTAT3+NPY double-label IHC. Data are expressed as means ± SE with average neuronal counts per section. *$P < 0.05$ or less, two-sample *t*-test.

sensitive neurons in DIO rats. In the presence of this amylin-induced increase in ARC leptin signaling, amylin-treated DIO neonates had a twofold increase in the density of both AgRP and α-MSH fibers in the PVN at P17 (AgRP: Fig. 6, *A–C*; α-MSH: Fig. 6, *D–F*). Whereas postnatal amylin treatment from P0 to P16 improved DIO ARC-PVN pathway development and caused them to gain 7% less body weight during the amylin administration (Fig. 5*A*), there were no sustained effects of treatment on body weight gain. After treatment cessation at P16, body weight gain in chow-fed, amylin-treated DIO neonates returned to that of control DIO rats by weaning at P21 (Fig. 5*A* and Table 1). Finally, despite the amylin-induced improvement in DIO ARC-PVN pathway development, this anatomic improvement had no sustained effect on lowering body weight gain once treatment was terminated.

Effects of P0–16 amylin treatment on DIO post-weaning VMH leptin signaling, energy and glucose homeostasis. To assess whether neonatal amylin treatment had a sustained effect on leptin signaling, energy, and glucose homeostasis in DIO rats, separate groups were treated with amylin or saline from P0 to P16, weaned onto chow at 3 wk of age and fed chow for a total of 5 wk. The previously demonstrated increase in the number of leptin-induced pSTAT3 neurons at P17 in DIO rats was maintained after 5 wk on chow, where there were 27% more ARC leptin-induced pSTAT3-positive neurons compared with controls (Fig. 7, *A–D*). On the other hand, there was no effect on VMN pSTAT3 expression (Fig. 7*C*) or on ARC or VMN leptin receptor binding (Fig. 7*D*). Despite their apparently enhanced leptin signaling (leptin-induced pSTAT3), neonatal amylin treatment did not improve the defective leptin–induced anorexia of DIO rats (12) at either 4 or 24 h (data not shown). Neonatal amylin treatment also had no effect on postweaning body weight gain, food intake, overall adiposity, or glucose and insulin responses to an OGTT over 5 wk on chow compared with controls (Table 1). Unexpectedly, prior amylin treatment was associated with a 40% increase in retroperitoneal fat pad weights and a 10% increase in liver weight as a percentage of carcass weight.

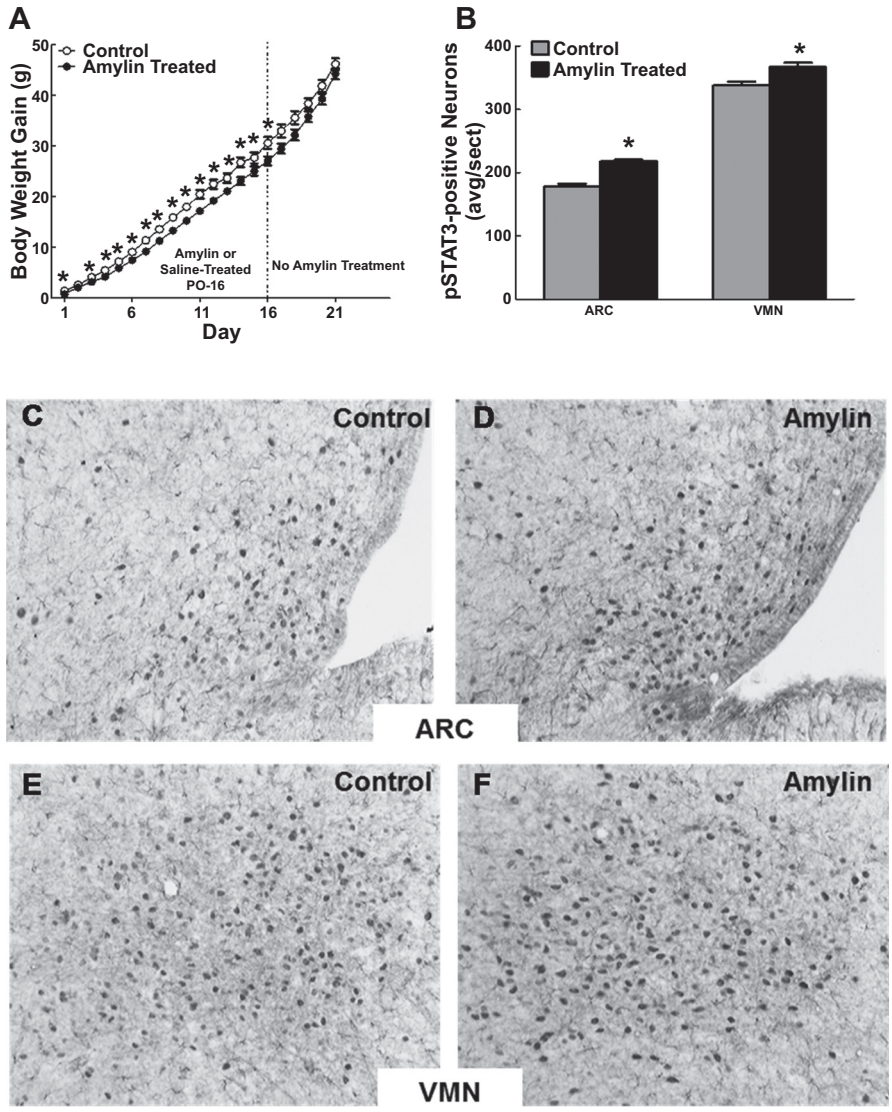

Fig. 5. Body weight gain from P0 to P21 (*A*) and leptin-induced pSTAT3 IHC (*B–F*) in P17 DIO neonates treated with amylin (P0–16, 300 μg ·kg^{-1} ·day^{-1}) vs. vehicle (0.9% saline). Data are expressed as means ± SE. Dotted line denotes cessation of postnatal treatment period. Images (×20) of leptin-induced pSTAT3 in ARC (*C*, Control; *D*, Amylin Treated) and VMN (*E*, Control; *F*, Amylin Treated). *$P < 0.05$ or less. *A*: one-way ANOVA with repeated measures and two-sample *t*-test for each data point; *B*: two-way ANOVA and two-sample *t*-test.

Effects of P0–16 amylin treatment on energy and glucose homeostasis in DIO rats fed HE diet as adults. To assess whether neonatal amylin treatment might provide long-term protection of DIO rats from becoming obese on HE diet, a separate group of DIO rats was treated with amylin or vehicle from P0 to P16, fed chow for 5 wk from weaning, and then fed HE diet for 8 wk more. As in amylin-treated chow-fed DIO rats, neonatal amylin treatment had no lasting effect on body weight gain, food intake, total carcass adiposity, or plasma leptin levels compared with controls after 8 wk on HE diet (Table 1). However, prior amylin treatment did result in a selective 22% increase in inguinal fat pad weights as a percentage of carcass weight compared with controls (Table 1). This suggests that neonatal amylin treatment might produce a redistribution of fat from visceral to subcutaneous depots. Despite this moderate increase in subcutaneous fat, neonatal amylin treatment produced no improvement in insulin sensitivity (glucose or insulin AUC during an OGTT or ISI) after 8 wk on HE diet (Table 1). However, amylin-treated DIO rats did have 33% lower fasting insulin levels compared with controls (Table 1).

Experiment 3: Requirement for IL-6 in ARC-PVN Pathway Development

We previously demonstrated that amylin administration increases VMH leptin signaling via an IL-6-dependent mechanism in adult rodents (18). The data presented here also indicate that neonatal amylin treatment improved the defective ARC-PVN AgRP and α-MSH pathway development in DIO rats (Fig. 6). To assess whether IL-6 signaling is required for normal ARC AgRP and α-MSH axon outgrowth to the PVN, we assessed the density of α-MSH and AgRP axon terminals in the PVN of P17 IL-6 KO vs. WT mice (Fig. 8). Similar to DIO rats (8), IL-6 KO mice had an approximately twofold reduction in PVN AgRP fiber density compared with WT mice (Fig. 8, *A–C*). However, unlike DIO rats (8), α-MSH PVN axonal density in IL-6 KO mice was comparable to that of WT mice (Fig. 8, *D–F*). These results suggest that AgRP ARC-PVN pathway outgrowth is IL-6 dependent, whereas α-MSH ARC-PVN pathway outgrowth is IL-6 independent. It also suggests that improvement in DIO AgRP, but not α-MSH, PVN axon density in amylin-treated DIO neonates might be IL-6 dependent.

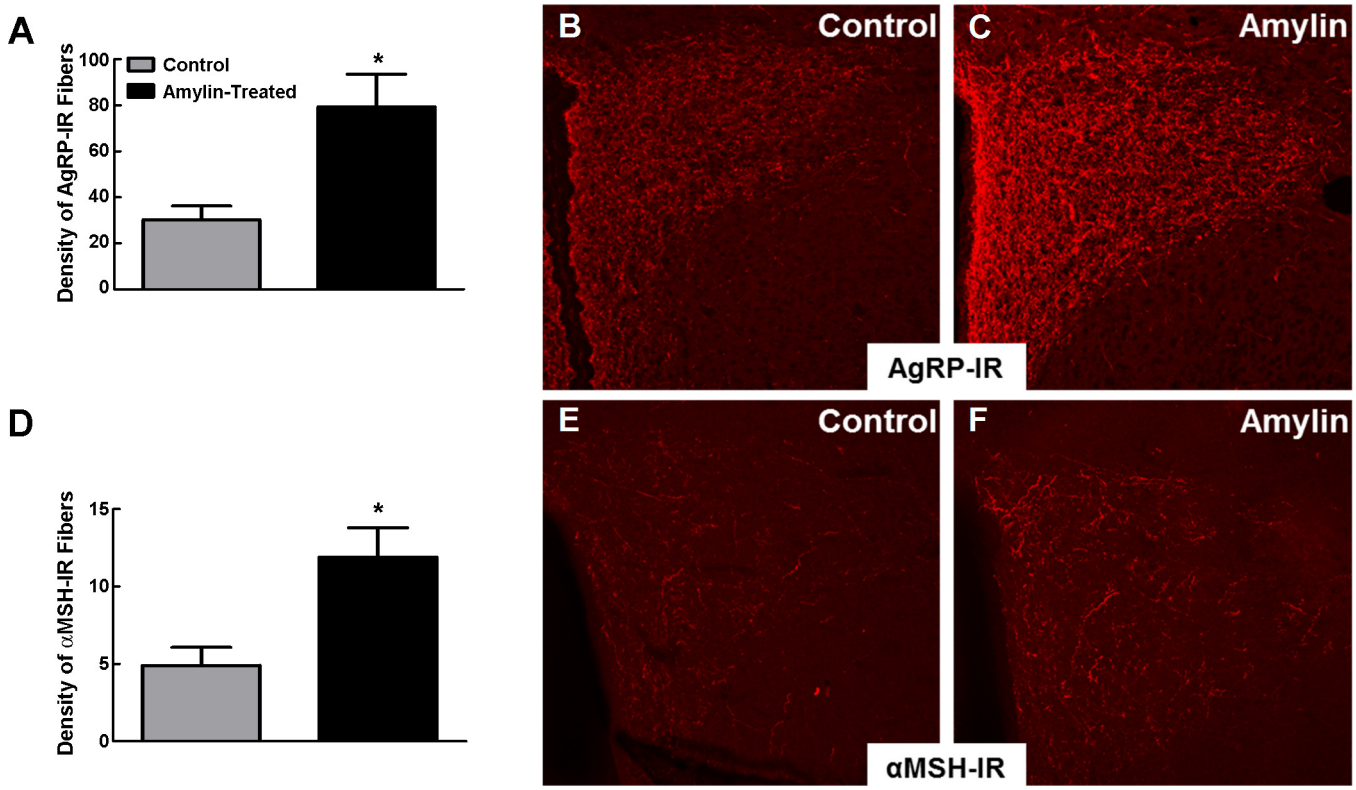

Fig. 6. AgRP and α-MSH ARC-PVN pathway development in P17 DIO neonates treated with amylin (300 μg ·kg^{-1} ·day^{-1}) vs. vehicle (0.9% saline) from P0 to P16. Data are expressed as means ± SE. Confocal images and quantification of AgRP- (*A–C*) and α-MSH-immunopositive positive axons (*D–F*) in the PVN. *$P < 0.05$ or less, two-sample *t*-test.

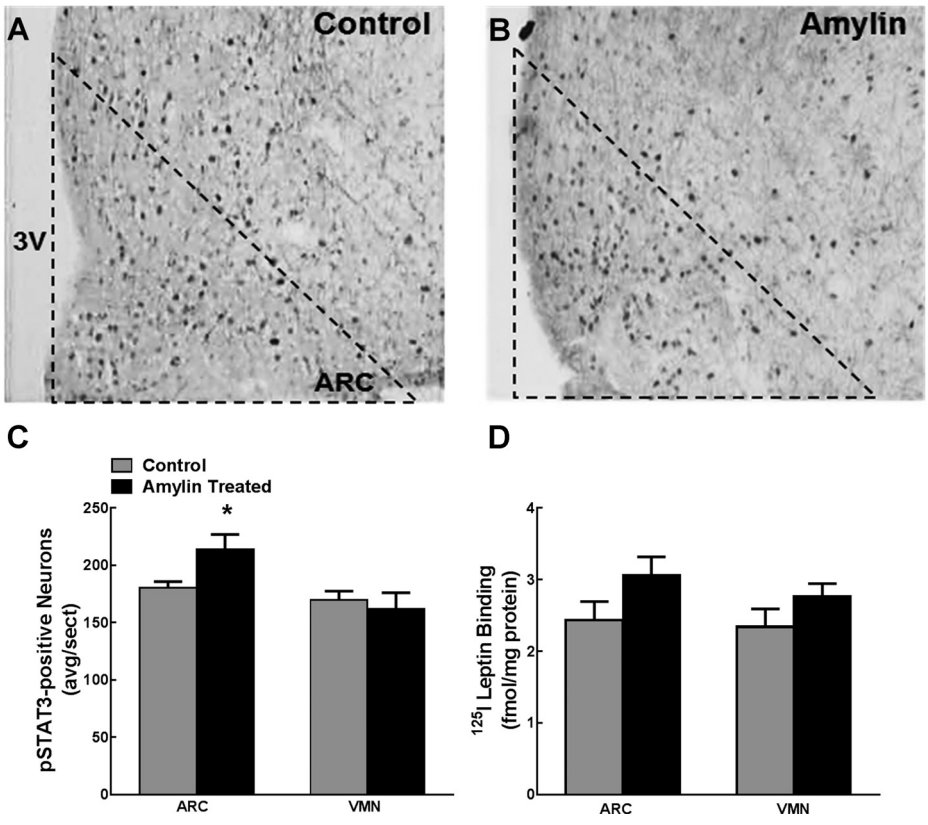

Fig. 7. Postweaning leptin receptor signaling and binding in DIO rats treated with amylin (300 μg ·kg^{-1} ·day^{-1}) vs. vehicle (0.9% saline) from P0 to P16 and then fed chow for 5 wk. *A–C*: ARC and VMN leptin-induced pSTAT3 IHC. Images (×20) of leptin-induced pSTAT3-positive neurons in the ARC of adult rats previously treated with vehicle (control; *A*) or amylin (*B*) as neonates. *D*: ARC and VMN ^{125}I-labeled leptin receptor binding. Data are expressed as means ± SE *$P < 0.05$ or less, two-way ANOVA and two-sample *t*-test.

Table 1. *Effects of neonatal amylin treatment vs. vehicle in DIO rats*

	Control	Amylin Treated
Neonatal period		
P0 body weight, g	7.2 ± 0.1	7.2 ± 0.2
P17 body weight, g	40.5 ± 0.5	38.1 ± 0.6*
P0−P17 body weight gain, g	33.3 ± 0.5	30.9 ± 0.5*
Weeks 1–5 chow		
Initial body weight *P21*, g	54 ± 1.4	53 ± 1.4
Body weight *week 5*, g	366 ± 5.3	353 ± 6.5
Body weight gain *week 1–5*, g	311 ± 5.0	300 ± 5.5
Food intake *week 1–5*, kcal	3,276 ± 77	3,242 ± 64
Feed efficiency *week 1–5* [(BWG (g)/FI (kcal)]×1,000)	94 ± 1	93 ± 1
Insulin *week 5*, ng/ml	1.41 ± 0.15	1.23 ± 0.13
Glucose *week 5*, mg/dl	163 ± 3.84	160 ± 3.61
OGTT insulin AUC *week 4*	63.8 ± 6.77	50.8 ± 5.35
OGTT glucose AUC *week 4*	3,137 ± 388	2,918 ± 326
Insulin sensitivity index	41.4 ± 3.0	50.4 ± 4.0
Leptin *week 5*, ng/ml	6.19 ± 0.73	7.40 ± 0.78
Retroperitoneal, g	2.1 ± 0.4	2.6 ± 0.3
Retroperitoneal, %body wt	0.5 ± 0.1	0.7 ± 0.1*
Mesenteric, g	3.4 ± 0.3	3.4 ± 0.3
Mesenteric, %body wt	0.9 ± 0.1	1.0 ± 0.1
Perirenal, g	0.5 ± 0.1	0.7 ± 0.1
Perirenal, %body wt	0.2 ± 0.02	0.2 ± 0.02
Epididymal, g	3.0 ± 0.4	2.8 ± 0.3
Epididymal, %body wt	0.8 ± 0.1	0.8 ± 0.1
Inguinal, g	3.0 ± 0.2	3.1 ± 0.1
Inguinal, %body wt	0.8 ± 0.1	0.9 ± 0.0
Total fat pad weight, g	11.1 ± 1.1	12.1 ± 0.9
Total body fat, %body wt	3.4 ± 0.3	3.5 ± 0.2
Liver, g	16.5 ± 0.8	16.0 ± 0.6
Liver, %body wt	4.1 ± 0.1	4.5 ± 0.1*
Weeks 6–13 HE diet		
Body weight *week 6*, g	362 ± 4.2	355 ± 6.5
Body weight gain *week 6–13*, g	335 ± 12.4	334 ± 6.9
Food intake *wk 6–13*, kcal	6,647 ± 222	6,982 ± 193
Feed efficiency *week 6–13* [(BWG (g)/FI (kcal)]×1,000	49 ± 1	49 ± 1
Weeks 1–13		
Final body weight, g	680 ± 23.1	699 ± 15.7
Body weight gain *week 1–13*, g	646 ± 19.4	645 ± 14.6
Food intake *week 1–13*, kcal	9,967 ± 239	10,228 ± 276
Feed efficiency *week 1–13* [(BWG (g)/FI (kcal)]×1,000)	64 ± 1	62 ± 1
Final insulin, ng/ml	4.20 ± 0.20	2.83 ± 0.10*
Final glucose, mg/dl	148 ± 4.89	153 ± 5.15
OGTT insulin AUC *week 12*	202 ± 66.7	296 ± 63.4
OGTT glucose AUC *week 12*	6,384 ± 1,752	3,673 ± 1,145
Insulin sensitivity index	12.5 ± 1.79	14.5 ± 1.20
Final leptin, ng/ml	39.1 ± 3.1	40.4 ± 2.9
Retroperitoneal, g	18.9 ± 1.3	22.2 ± 0.6
Retroperitoneal, %body wt	3.1 ± 0.3	3.6 ± 0.5
Mesenteric, g	19.9 ± 1.3	23.2 ± 1.4
Mesenteric, %body wt	3.0 ± 0.1	3.3 ± 0.1
Perirenal, g	8.5 ± 1.2	7.9 ± 1.2
Perirenal, %body wt	1.2 ± 0.2	1.1 ± 0.2
Epididymal, g	22.2 ± 1.3	21.6 ± 2.2
Epididymal, %body wt	3.3 ± 0.1	3.1 ± 0.3
Inguinal, g	20.4 ± 1.0	27.4 ± 0.4*
Inguinal, %body wt	3.2 ± 0.1	3.9 ± 0.1*
Total fat pad weight, g	95 ± 6.4	106 ± 5.3
Total body fat, %body wt	13.9 ± 0.5	14.9 ± 0.3
Liver, g	20.8 ± 1.0	22.2 ± 1.2
Liver, %body wt	3.1 ± 0.1	3.2 ± 0.2

Data are expressed as means ± SE. Diet-induced obese rats treated with amylin (300 $\mu g \cdot kg^{-1} \cdot day^{-1}$) or saline (0.9%) from P0 to P16 and fed chow for 5 wk at weaning and then high-energy diet for 8 wk. OGTT, oral glucose tolerance test; BWG, body weight gain; FI, food intake. Insulin sensitivity index = 10,000/Sqrt (fasting glucose × fasting insulin) × (mean glucose × mean insulin) (29). *$P < 0.05$, two-sample *t*-test.

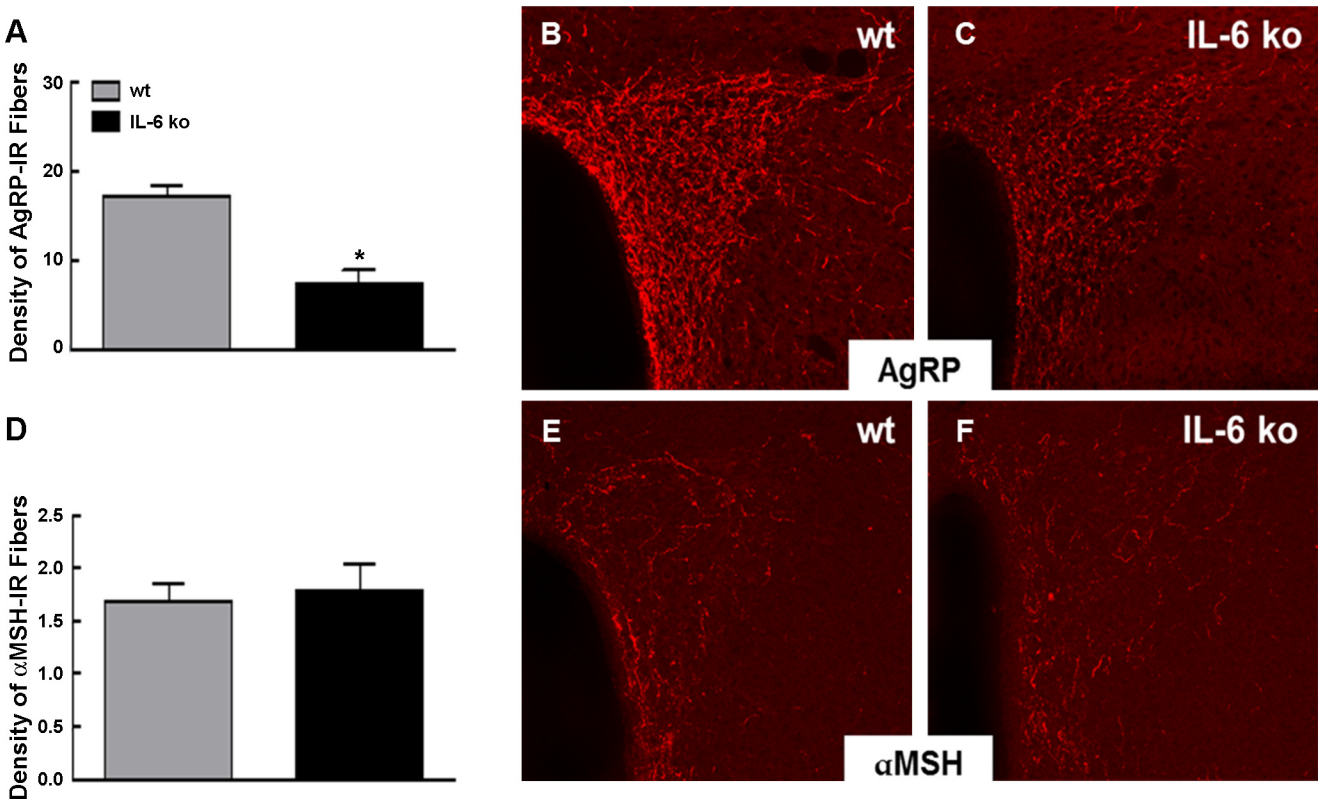

Fig. 8. AgRP and α-MSH ARC-PVN pathway development in P17 IL-6 KO and WT mice. Data are expressed as means ± SE. Confocal images and quantification of AgRP- (*A–C*) and α-MSH-immunopositive axons (*D–F*) in the PVN. *$P < 0.05$ or less, two-sample *t*-test.

DISCUSSION

We previously reported that the DIO rat has impaired leptin responsiveness in the ARC at P10 and decreased leptin-dependent ARC-PVN neurite outgrowth (8). Here, we show that ARC leptin signaling, using leptin-induced pSTAT3 as a surrogate, occurs in DIO and DR neonates at birth, and that decreased leptin signaling occurs in DIO rats by P7. Therefore, leptin resistance does not appear to be an inborn trait of the DIO rat. Moreover, this decrease in leptin signaling occurred in a select subpopulation of ARC POMC neurons located in the mid-part of the ARC but occurred in none of the ARC NPY/AgRP neurons. Although ARC NPY neuron number was reduced in DIO neonates at birth, this difference did not persist at later ages. Next, since exogenous administration of amylin has been shown to increase ARC and VMN leptin signaling in adult rats (35, 45), we hypothesized that postnatal treatment with amylin from P0 to P6 might improve ARC leptin signaling during the first week of postnatal life. In fact, 7 days of postnatal amylin treatment increased ARC leptin signaling and increased the number of rostral POMC neurons. But this response appeared to be leptin independent, since there was no increase in the number of leptin-sensitive POMC neurons. In addition, much of the amylin-induced increase in the number of leptin-sensitive ARC neurons at P7 in DIO rats appears to have occurred in other neuronal populations than POMC or NPY neurons. Because the amylin-induced increase of leptin signaling has been shown to be mediated by IL-6 in adults (18), we postulated that IL-6 might also be a key regulator of the amylin-induced enhancement of DIO neonatal ARC-PVN pathway development which we demonstrated here. Surprisingly, IL-6 KO mice had only impaired AgRP, but not α-MSH ARC-PVN pathway development. Taken together with the finding that early neonatal amylin treatment increased only the total number of ARC POMC, but not leptin-sensitive POMC or leptin-sensitive or -insensitive NPY neurons, these data collectively suggest that amylin might have a leptin-independent neurotrophic effect selectively on POMC neuron birth, migration and/or apoptosis and axon outgrowth during early postnatal hypothalamic development.

Once ARC POMC and NPY/AgRP neurons reach their final anatomic locations, they send out axons to targets in the PVN and other hypothalamic nuclei during the first two weeks of postnatal life in rodents (6). ARC-PVN pathway development for α-MSH and AgRP neurons is leptin dependent, and early neonatal amylin treatment increased both in the DIO rat. In addition, amylin acts to enhance VMH leptin signaling via an IL-6-dependent mechanism (18), but IL-6 KO mice have defective AgRP, but not α-MSH, pathway development, suggesting a more complex interaction between amylin and leptin on this pathway. For AgRP ARC-PVN pathway development, amylin-induced enhancement might be leptin dependent, given the dependence of amylin-induced enhancement of VMH leptin signaling on IL-6 (18). In contrast, for α-MSH ARC-PVN pathway development, amylin appeared to enhance development in DIO rats by both leptin- and IL-6-independent mechanisms, since IL-6 KO mice had normal α-MSH ARC-PVN pathways. Of course, some of these differences might represent

those imposed by endogenous amylin signaling as opposed to exogenous amylin administration (23). Thus, although we have demonstrated that exogenous amylin, administered early in postnatal life, can greatly ameliorate the reduced number of ARC leptin-sensitive neurons (most of which at P7 are neither POMC nor NPY/AgRP neurons) and outgrowth of axons from ARC POMC and NPY/AgRP neurons in DIO rats, it is likely that some of these effects are independent of the amylin-IL-6 enhancement of leptin signaling seen in adult rats.

Another important finding is that, while postnatal amylin treatment enhanced ARC leptin signaling and pathway development in DIO rats, it had no sustained effect on protecting them from becoming obese when fed a moderate-fat HE diet as adults. In part, this lack of long-term protection might be due to the lack of correction of the defective binding of leptin to its receptors in the ARC and VMN (16). Perhaps the most important finding is that rescue of anatomic pathway defects in DIO rats alone is insufficient to provide them with sustained protection from development of diet-induced obesity.

We found that there was a dynamic change in the numbers of both POMC and NPY neurons in the four divisions of the ARC during the first week of postnatal life in both DIO and DR neonates. Across all ages examined, there was a generalized increase in the number of POMC and NPY neurons in both DIO and DR rats. This increase could represent an increase in neurogenesis, migration of neurons from the tanycyte layer (19, 48) and/or migration from one division to another, and/or a decrease in apoptosis. Even in the adult rodents, there appears to be continued neurogenesis of ARC POMC neurons (19). Leptin has been demonstrated to affect migration of cerebral cortical neurons (46), whereas no clear effect of leptin on either neurogenesis or neuronal apoptosis has been described to date. However, our studies demonstrate that exogenous neonatal amylin administration has a selective effect on increasing the number of both leptin-sensitive ARC neurons and leptin-insensitive POMC neurons, as well as improving the outgrowth of axons from both POMC and NPY/AgRP neurons to their targets. Amylin administration has been shown to increase neurogenesis in the AP and hippocampus (24, 44).

We previously demonstrated that exogenous amylin acts to improve VMH leptin signaling by stimulating microglia to produce IL-6, which then acts through its IL-6 receptor/gp130 complex to activate STAT3 (18). This is the likely mechanism by which amylin enhances VMH leptin signaling to provide a synergistic effect on weight loss in obese DIO rats and humans (35, 45). Amylin treatment in DIO neonates improved both α-MSH and AgRP ARC-PVN pathway development and increased the number of rostral ARC POMC neurons. However, since IL-6 KO mice had defective development of only the AgRP pathway, amylin-induced improvement of ARC POMC neuronal outgrowth may not be IL-6 dependent, as α-MSH projections were not affected in the absence of IL-6. This suggests that amylin might act by two independent mechanisms: AgRP being IL-6 dependent and α-MSH being IL-6 independent (Fig. 9). While others have reported that IL-6-treated ARC explants had reduced neurite outgrowth, this could be due to exogenous IL-6 dose (36), as we show here that lack of IL-6 in KO mice resulted in adverse hypothalamic pathway development. Also, because exogenous amylin treatment did not affect leptin signaling in POMC neurons, this suggests that amylin's effect on outgrowth of α-MSH axons

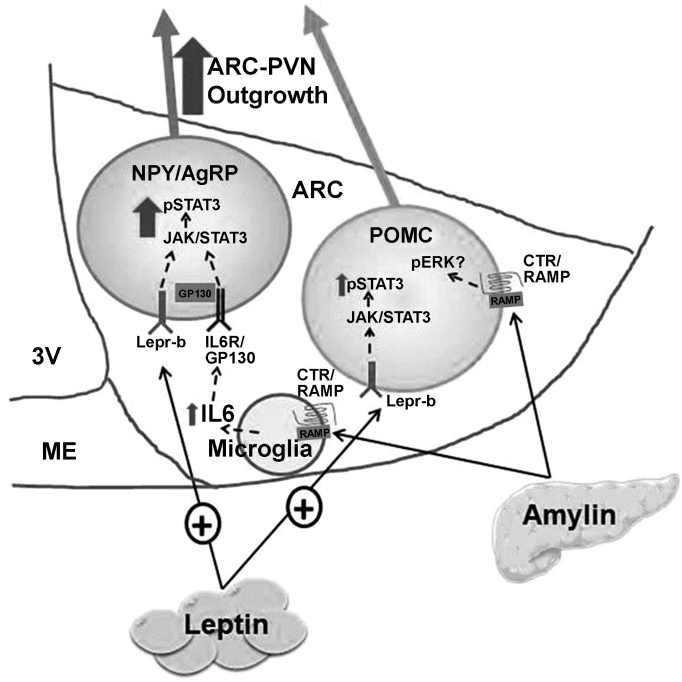

Fig. 9. Hypothetical model for mechanisms of amylin's actions to promote AgRP/NPY and α-MSH ARC-PVN outgrowth. Images of pancreas and adipocytes modified from (37; Powerpoint Image Bank Servier Medical Art. 2016. CC BY-NC 3.0, http://www.servier.com/Powerpointimage-bank).

from POMC neurons might be through a direct neurotrophic mechanism that is leptin independent, possibly through the MAP kinase/phospho-ERK pathway by which amylin activates AP neurons to promote satiety (32). A role for endogenous amylin signaling in neuronal pathway development is also supported by preliminary data suggesting that amylin KO mice have reduced AP-nucleus of the solitary tract (NTS) pathway development (27). A potential caveat of our findings is that 7 days of amylin treatment did not increase leptin signaling within NPY-positive neurons. Since amylin increased the density of AgRP-positive fibers in the PVN, and NPY has been shown to colocalize with ≥95% of AgRP neurons in the ARC (13, 39), a likely explanation for these findings could be that 7 days was insufficient to increase leptin signaling, whereas DIO neonates treated with amylin from P0 to P16 may have shown an increased number of pSTAT3-NPY-positive neurons.

There appears to be an important difference between the actions of exogenous amylin administration on short- vs. long-term reductions in food intake and body weight in lean and obese rodents and/or humans (34, 35). The short-term satiating effects of amylin appear to be mediated by an ERK-dependent mechanism in the AP/NTS (4, 28, 32), while the longer-term reductions in intake and body weight of exogenous amylin may be mediated by its stimulation of leptin signaling in the ARC and VMN (18, 45). Thus, although we did not measure meal size or duration, the small decrease in body weight seen here during amylin administration was likely mediated by its direct effects on the AP/NTS, since there was a rapid return of body weight to control levels after discontinuance of amylin treatment. Additionally, there may be an important difference between the effects of exogenous amylin administration and endogenous amylin signaling. Thus, while postnatal amylin

treatment improved ARC AgRP and α-MSH pathway development, this alone was insufficient to protect DIO rats from becoming obese as adults when placed on HE diet. Recently, we (10) showed that disrupting endogenous VMN amylin signaling through depletion of the CTR component of the amylin receptor complex resulted in increased body weight gain, plasma leptin levels, and decreased leptin signaling and binding in the ARC and/or VMN. In addition, adult DIO rats have reduced ^{125}I-labeled amylin binding in the VMN (18). While postnatal amylin treatment of DIO neonates increased their ARC leptin signaling and development of their ARC-PVN pathway, their reduced VMN amylin and leptin signaling might promote their obese phenotype on HE diet.

Perspectives and Significance

While amylin has been well studied for its role in regulating energy homeostasis, our current studies demonstrate a novel role for amylin in altering both the number of ARC POMC and other leptin-responsive neurons and improving the defective outgrowth of both α-MSH and AgRP axons to the PVN when administered to leptin-resistant DIO neonates during the first 7–16 days of postnatal life. Despite this improvement in neuronal numbers and pathway development, amylin had no persistent effects on weight gain after cessation of treatment. This supports the notion that improvement of this pathway, particularly if it equally affects both catabolic α-MSH and anabolic AgRP pathways in the DIO rat, is not the critical determinant of future propensity to become obese on energy-dense diets if the underlying leptin resistance is not also corrected. Finally, we have shown that outgrowth of α-MSH and AgRP axons is differentially dependent on the presence of IL-6, a factor that we previously demonstrated to be a critical component of amylin's ability to enhance ARC leptin signaling (18). While AgRP axonal outgrowth is leptin dependent in DIO rats (8) and mice (7), it also appears to depend on the presence of IL-6 (and by inference, on amylin signaling) for full expression. On the other hand, the lack of IL-6 dependence of α-MSH pathway development, but marked improvement to amylin in DIO rats, suggests that this response might be due to a direct effect of amylin on leptin-responsive neurons by activating ERK and cAMP, as occurs in AP neurons (40). Thus, the present studies demonstrate novel roles for amylin and amylin-leptin interactions on hypothalamic development and leptin signaling. These findings provide strong support for amylin as an important mediator of both energy homeostasis and neuronal development.

ACKNOWLEDGMENTS

We thank Charlie Salter, Antoinette Moralishvili, and Sunny Lee for their expert technical assistance.

GRANTS

This work was funded by the Research Service of the Veterans Administration (BEL, AAD-M), NIDDK-DK R01–30066 (BEL), American Heart Association (MDJ), Swiss National Science Foundation, and the Center for Integrative Human Physiology (TAL), NIDDK DK-84142 and DK-102780 (SGB).

DISCLOSURES

No conflicts of interest, financial or otherwise, are declared by the author(s).

AUTHOR CONTRIBUTIONS

M.D.J., A.A.D.-M., T.A.L., and B.E.L. conception and design of research; M.D.J., S.G.B., and A.A.D.-M. performed experiments; M.D.J., S.G.B., A.A.D.-M., C.N.B., and B.E.L. analyzed data; M.D.J., A.A.D.-M., C.N.B., T.A.L., and B.E.L. interpreted results of experiments; M.D.J. and S.G.B. prepared figures; M.D.J. drafted manuscript; M.D.J., T.A.L., and B.E.L. edited and revised manuscript; M.D.J., S.G.B., A.A.D.-M., C.N.B., T.A.L., and B.E.L. approved final version of manuscript.

REFERENCES

1. **Banks WA, Kastin AJ.** Differential permeability of the blood-brain barrier to two pancreatic peptides: insulin and amylin. *Peptides* 19: 883–889, 1998. doi:10.1016/S0196-9781(98)00018-7.
2. **Banks WA, Kastin AJ, Maness LM, Huang W, Jaspan JB.** Permeability of the blood-brain barrier to amylin. *Life Sci* 57: 1993–2001, 1995. doi:10.1016/0024-3205(95)02197-Q.
3. **Baquero AF, de Solis AJ, Lindsley SR, Kirigiti MA, Smith MS, Cowley MA, Zeltser LM, Grove KL.** Developmental switch of leptin signaling in arcuate nucleus neurons. *J Neurosci* 34: 9982–9994, 2014. doi:10.1523/JNEUROSCI.0933-14.2014.
4. **Barth SW, Riediger T, Lutz TA, Rechkemmer G.** Peripheral amylin activates circumventricular organs expressing calcitonin receptor a/b subtypes and receptor-activity modifying proteins in the rat. *Brain Res* 997: 97–102, 2004. doi:10.1016/j.brainres.2003.10.040.
5. **Becskei C, Riediger T, Zünd D, Wookey P, Lutz TA.** Immunohistochemical mapping of calcitonin receptors in the adult rat brain. *Brain Res* 1030: 221–233, 2004. doi:10.1016/j.brainres.2004.10.012.
6. **Bouret SG, Draper SJ, Simerly RB.** Formation of projection pathways from the arcuate nucleus of the hypothalamus to hypothalamic regions implicated in the neural control of feeding behavior in mice. *J Neurosci* 24: 2797–2805, 2004. doi:10.1523/JNEUROSCI.5369-03.2004.
7. **Bouret SG, Draper SJ, Simerly RB.** Trophic action of leptin on hypothalamic neurons that regulate feeding. *Science* 304: 108–110, 2004. doi:10.1126/science.1095004.
8. **Bouret SG, Gorski JN, Patterson CM, Chen S, Levin BE, Simerly RB.** Hypothalamic neural projections are permanently disrupted in diet-induced obese rats. *Cell Metab* 7: 179–185, 2008. doi:10.1016/j.cmet.2007.12.001.
9. **Caron E, Sachot C, Prevot V, Bouret SG.** Distribution of leptin-sensitive cells in the postnatal and adult mouse brain. *J Comp Neurol* 518: 459–476, 2010. doi:10.1002/cne.22219.
10. **Dunn-Meynell AA, Le Foll C, Johnson MD, Lutz TA, Hayes MR, Levin BE.** Endogenous VMH amylin signaling is required for full leptin signaling and protection from diet-induced obesity. *Am J Physiol Regul Integr Comp Physiol* 310: R355–R365, 2016. doi:10.1152/ajpregu.00462.2015.
11. **Gorski JN, Dunn-Meynell AA, Hartman TG, Levin BE.** Postnatal environment overrides genetic and prenatal factors influencing offspring obesity and insulin resistance. *Am J Physiol Regul Integr Comp Physiol* 291: R768–R778, 2006. doi:10.1152/ajpregu.00138.2006.
12. **Gorski JN, Dunn-Meynell AA, Levin BE.** Maternal obesity increases hypothalamic leptin receptor expression and sensitivity in juvenile obesity-prone rats. *Am J Physiol Regul Integr Comp Physiol* 292: R1782–R1791, 2007. doi:10.1152/ajpregu.00749.2006.
13. **Hahn TM, Breininger JF, Baskin DG, Schwartz MW.** Coexpression of Agrp and NPY in fasting-activated hypothalamic neurons. *Nat Neurosci* 1: 271–272, 1998. doi:10.1038/1082.
14. **Hay DL, Christopoulos G, Christopoulos A, Sexton PM.** Amylin receptors: molecular composition and pharmacology. *Biochem Soc Trans* 32: 865–867, 2004. doi:10.1042/BST0320865.
15. **Higuchi H, Yang H-YT, Sabol SL.** Rat neuropeptide Y precursor gene expression. mRNA structure, tissue distribution, and regulation by glucocorticoids, cyclic AMP, and phorbol ester. *J Biol Chem* 263: 6288–6295, 1988.
16. **Irani BG, Dunn-Meynell AA, Levin BE.** Altered hypothalamic leptin, insulin, and melanocortin binding associated with moderate-fat diet and predisposition to obesity. *Endocrinology* 148: 310–316, 2007. doi:10.1210/en.2006-1126.
17. **Kahn SE, D'Alessio DA, Schwartz MW, Fujimoto WY, Ensinck JW, Taborsky GJ Jr, Porte D Jr.** Evidence of cosecretion of islet amyloid polypeptide and insulin by beta-cells. *Diabetes* 39: 634–638, 1990. doi:10.2337/diab.39.5.634.
18. **Le Foll C, Johnson MD, Dunn-Meynell AA, Boyle CN, Lutz TA, Levin BE.** Amylin-induced central IL-6 production enhances ventromedial hy-

pothalamic leptin signaling. *Diabetes* 64: 1621–1631, 2015. doi:10.2337/db14-0645.

19. **Lee DA, Bedont JL, Pak T, Wang H, Song J, Miranda-Angulo A, Takiar V, Charubhumi V, Balordi F, Takebayashi H, Aja S, Ford E, Fishell G, Blackshaw S.** Tanycytes of the hypothalamic median eminence form a diet-responsive neurogenic niche. *Nat Neurosci* 15: 700–702, 2012. doi:10.1038/nn.3079.
20. **Levin BE, Dunn-Meynell AA, Balkan B, Keesey RE.** Selective breeding for diet-induced obesity and resistance in Sprague-Dawley rats. *Am J Physiol* 273: R725–R730, 1997.
21. **Levin BE, Dunn-Meynell AA, Banks WA.** Obesity-prone rats have normal blood-brain barrier transport but defective central leptin signaling before obesity onset. *Am J Physiol Regul Integr Comp Physiol* 286: R143–R150, 2003. doi:10.1152/ajpregu.00393.2003.
22. **Levin BE, Dunn-Meynell AA, Ricci MR, Cummings DE.** Abnormalities of leptin and ghrelin regulation in obesity-prone juvenile rats. *Am J Physiol Endocrinol Metab* 285: E949–E957, 2003. doi:10.1152/ajpendo.00186.2003.
23. **Li Z, Kelly L, Gergi I, Vieweg P, Heiman M, Greengard P, Friedman JM.** Hypothalamic Amylin Acts in Concert with Leptin to Regulate Food Intake. *Cell Metab* 22: 1059–1067, 2015. doi:10.1016/j.cmet.2015.10.012.
24. **Liberini CG, Borner T, Boyle CN, Lutz TA.** The satiating hormone amylin enhances neurogenesis in the area postrema of adult rats. *Mol Metab* 5: 834–843, 2016. doi:10.1016/j.molmet.2016.06.015.
25. **Liberini CG, Boyle CN, Cifani C, Venniro M, Hope BT, Lutz TA.** Amylin receptor components and the leptin receptor are co-expressed in single rat area postrema neurons. *Eur J Neurosci* 43: 653–661, 2016. doi:10.1111/ejn.13163.
26. **Lutz TA.** Amylinergic control of food intake. *Physiol Behav* 89: 465–471, 2006. doi:10.1016/j.physbeh.2006.04.001.
27. **Lutz TA.** The role of amylin in the control of energy homeostasis. *Am J Physiol Regul Integr Comp Physiol* 298: R1475–R1484, 2010. doi:10.1152/ajpregu.00703.2009.
28. **Lutz TA, Mollet A, Rushing PA, Riediger T, Scharrer E.** The anorectic effect of a chronic peripheral infusion of amylin is abolished in area postrema/nucleus of the solitary tract (AP/NTS) lesioned rats. *Int J Obes Relat Metab Disord* 25: 1005–1011, 2001. doi:10.1038/sj.ijo.0801664.
29. **Matsuda M, DeFronzo RA.** Insulin sensitivity indices obtained from oral glucose tolerance testing: comparison with the euglycemic insulin clamp. *Diabetes Care* 22: 1462–1470, 1999. doi:10.2337/diacare.22.9.1462.
30. **Palkovits M.** Stereotaxic Map, Cytoarchitectonic and Neurochemical Summary of the Hypothalamic Nuclei, in *Endocrine System* (Jones T, Mohr U, Hunt R, Capen C, editors). Berlin, Heidelberg: Springer, 1983, p. 316–331. doi:10.1007/978-3-642-96720-7_64
31. **Patterson CM, Bouret SG, Park S, Irani BG, Dunn-Meynell AA, Levin BE.** Large litter rearing enhances leptin sensitivity and protects selectively bred diet-induced obese (DIO) rats from becoming obese. *Endocrinology* 151: 4270–4279, 2010. doi:10.1210/en.2010-0401.
32. **Potes CS, Boyle CN, Wookey PJ, Riediger T, Lutz TA.** Involvement of the extracellular signal-regulated kinase 1/2 signaling pathway in amylin's eating inhibitory effect. *Am J Physiol Regul Integr Comp Physiol* 302: R340–R351, 2012. doi:10.1152/ajpregu.00380.2011.
33. **Ricci MR, Levin BE.** Ontogeny of diet-induced obesity in selectively bred Sprague-Dawley rats. *Am J Physiol Regul Integr Comp Physiol* 285: R610–R618, 2003. doi:10.1152/ajpregu.00235.2003.
34. **Roth JD, Hughes H, Kendall E, Baron AD, Anderson CM.** Antiobesity effects of the beta-cell hormone amylin in diet-induced obese rats: effects on food intake, body weight, composition, energy expenditure, and gene expression. *Endocrinology* 147: 5855–5864, 2006. doi:10.1210/en.2006-0393.
35. **Roth JD, Roland BL, Cole RL, Trevaskis JL, Weyer C, Koda JE, Anderson CM, Parkes DG, Baron AD.** Leptin responsiveness restored by amylin agonism in diet-induced obesity: evidence from nonclinical and clinical studies. *Proc Natl Acad Sci USA* 105: 7257–7262, 2008. doi:10.1073/pnas.0706473105.
36. **Sanders TR, Kim DW, Glendining KA, Jasoni CL.** Maternal obesity and IL-6 lead to aberrant developmental gene expression and deregulated neurite growth in the fetal arcuate nucleus. *Endocrinology* 155: 2566–2577, 2014. doi:10.1210/en.2013-1968.
37. **Servier Medical Art.** Powerpoint Image Bank Servier Medical Art. *Mumbai: Serdia Pharmaceuticals. 2016*. http://www.servier.com/Powerpoint-image-bank
38. **Sexton PM, Paxinos G, Kenney MA, Wookey PJ, Beaumont K.** In vitro autoradiographic localization of amylin binding sites in rat brain. *Neuroscience* 62: 553–567, 1994. doi:10.1016/0306-4522(94)90388-3.
39. **Shutter JR, Graham M, Kinsey AC, Scully S, Lüthy R, Stark KL.** Hypothalamic expression of ART, a novel gene related to agouti, is up-regulated in obese and diabetic mutant mice. *Genes Dev* 11: 593–602, 1997. doi:10.1101/gad.11.5.593.
40. **Smith PM, Brzezinska P, Hubert F, Mimee A, Maurice DH, Ferguson AV.** Leptin influences the excitability of area postrema neurons. *Am J Physiol Regul Integr Comp Physiol* 310: R440–R448, 2016. doi:10.1152/ajpregu.00326.2015.
41. **Steculorum SM, Collden G, Coupe B, Croizier S, Lockie S, Andrews ZB, Jarosch F, Klussmann S, Bouret SG.** Neonatal ghrelin programs development of hypothalamic feeding circuits. *J Clin Invest* 125: 846–858, 2015. doi:10.1172/JCI73688.
42. **Tkacs NC, Dunn-Meynell AA, Levin BE.** Presumed apoptosis and reduced arcuate nucleus neuropeptide Y and pro-opiomelanocortin mRNA in non-coma hypoglycemia. *Diabetes* 49: 820–826, 2000. doi:10.2337/diabetes.49.5.820.
43. **Trevaskis JL, Coffey T, Cole R, Lei C, Wittmer C, Walsh B, Weyer C, Koda J, Baron AD, Parkes DG, Roth JD.** Amylin-mediated restoration of leptin responsiveness in diet-induced obesity: magnitude and mechanisms. *Endocrinology* 149: 5679–5687, 2008. doi:10.1210/en.2008-0770.
44. **Trevaskis JL, Turek VF, Wittmer C, Griffin PS, Wilson JK, Reynolds JM, Zhao Y, Mack CM, Parkes DG, Roth JD.** Enhanced amylin-mediated body weight loss in estradiol-deficient diet-induced obese rats. *Endocrinology* 151: 5657–5668, 2010. doi:10.1210/en.2010-0590.
45. **Turek VF, Trevaskis JL, Levin BE, Dunn-Meynell AA, Irani B, Gu G, Wittmer C, Griffin PS, Vu C, Parkes DG, Roth JD.** Mechanisms of amylin/leptin synergy in rodent models. *Endocrinology* 151: 143–152, 2010. doi:10.1210/en.2009-0546.
46. **Udagawa J, Hashimoto R, Hioki K, Otani H.** The role of leptin in the development of the cortical neuron in mouse embryos. *Brain Res* 1120: 74–82, 2006. doi:10.1016/j.brainres.2006.08.116.
47. **Ueda T, Ugawa S, Saishin Y, Shimada S.** Expression of receptor-activity modifying protein (RAMP) mRNAs in the mouse brain. *Brain Res Mol Brain Res* 93: 36–45, 2001. doi:10.1016/S0169-328X(01)00179-6.
48. **Xu Y, Tamamaki N, Noda T, Kimura K, Itokazu Y, Matsumoto N, Dezawa M, Ide C.** Neurogenesis in the ependymal layer of the adult rat 3rd ventricle. *Exp Neurol* 192: 251–264, 2005. doi:10.1016/j.expneurol.2004.12.021.